Eur. Phys. J. B **14**, 449–458 (2000)

THE EUROPEAN PHYSICAL JOURNAL B

EDP Sciences

The fluid-solid transition of Dzugutov's potential

J. Roth[a]

Institut für Theoretische und Angewandte Physik, Universität Stuttgart, Pfaffenwaldring 57, 70550 Stuttgart, Germany

Received 15 June 1998 and Received in final form 8 July 1999

Abstract. We have studied fluid-solid phase transformations of materials interacting *via* the Dzugutov potential $V_{\mathrm{Dz}}(r)$ (Phys. Rev. A **46**, R2984 (1992)). We present evidence from molecular dynamics simulations that this interaction does not exhibit a liquid phase. If a mixed potential $V_{\mathrm{mix}}(\mathrm{r})$ is formed by a linear superposition of $V_{\mathrm{Dz}}(r)$ and the Lennard-Jones potential $V_{\mathrm{LJ}}(r)$, then the liquid phase disappears at a fraction of less than 60% $V_{\mathrm{LJ}}(r)$.

PACS. 61.44.Br Quasicrystals – 61.20.Ja Computer simulation of liquid structure

1 Introduction

It is well known that pair potentials with an attractive part (for example the Lennard-Jones potential), exhibit three different phases in the neighborhood of a triple point: a solid, a liquid, and a vapor phase. The temperature interval where the liquid phase exists (between the triple point and the critical point) depends on the range of the potential interaction: the shorter the range of the potential the smaller the domain will be. It is even possible that there is no liquid state if the potential is too short ranged. Such a behavior has recently been confirmed by analytical calculations [1–3] and by computer simulations [4–6] for hard spheres with additional attractive square-well [1,2,5], attractive Yukawa potentials [4,6], inverse power [1], and double Yukawa interactions [3]. In all the models the liquid phase disappears if the potential range is too short.

A common feature of the potentials treated in these papers is a repulsive core and an attractive well. The Dzugutov potential considered here is different, since it has a maximum between nearest and second nearest neighbors in addition to the minimum for nearest neighbors. Thus the potential loosely resembles the effective pair potentials used for metal interactions, but with the Friedel oscillations cut off after the first oscillation.

The Dzugutov potential [7] has recently gained interest in colloid science. By varying charges and polymer coatings of the colloid spheres it is possible to model a wide range of potential types. Since Dzugutov [8] discovered that his potential yields a stable quasicrystal it seems to be feasible to produce macroscopic quasicrystals experimentally. But before such an attempt is carried out one would like to gather as much insight as possible into the phase diagram of the Dzugutov potential.

[a] e-mail: johannes@itap.physik.uni-stuttgart.de

Further impetus to compute the phase diagram comes from our studies of quasicrystals. We have used the Dzugutov potential to simulate diffusion behavior [9–11] by molecular dynamics. Dzugutov has kept the volume constant in his cooling simulations. Thus he always got condensed phases. We have applied constant pressure instead of constant volume. In this case the system behaves completely different: it may not form a condensed phase at all if the pressure is too low.

The purpose of this paper is to present the melting and condensation behavior of the Dzugutov potential in some detail. A study of the solid phase is presented in a separate paper [12]. First the potential, the simulation setup, and the method to determine the phase boundaries are described (Sect. 2). Then the heating and expansion simulations are presented. The results indicate rather clearly that a liquid phase does not exist (Sect. 3). More evidence for the absence of the liquid phase is provided by a superposition of the Lennard-Jones potential and the Dzugutov potential (Sect. 4). The Lennard-Jones potential is chosen since its phase diagram is well known and a liquid phase exists. Furthermore, the Dzugutov potential has been derived from the Lennard-Jones potential. The simulations show that the liquid phase disappears if the contribution of the Lennard-Jones potential to the mixed potential is less than 60%. The paper is completed by a discussion and the conclusions in the final section (Sect. 5).

2 Models and methods

A new potential

Dzugutov recently has proposed a new simple pair potential which can be used to study glass transitions in a monoatomic system (see Fig. 1). The potential is given by

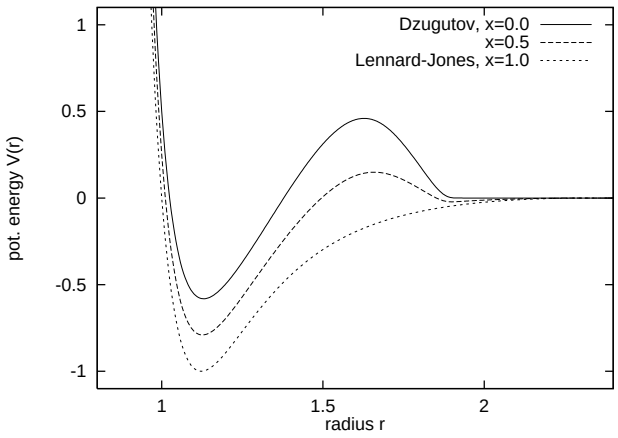

Fig. 1. Mixed Lennard-Jones–Dzugutov potentials $V(r) = xV_{\mathrm{LJ}}(r) + (1-x)V_{\mathrm{Dz}}(r)$.

the following equations:

$$V = V_1 + V_2$$
$$V_1 = A(r^{-m} - B)\exp\left(\frac{c}{r-a}\right), r < a,$$
$$V_1 = 0, r \geq a,$$
$$V_2 = B\exp\left(\frac{d}{r-b}\right), r < b,$$
$$V_2 = 0, r \geq b.$$

The parameters are:

m	A	c	a	B	d	b
16	5.82	1.1	1.87	1.28	0.27	1.94

The repulsive core of the potential is the same as the short-range part of the Lennard-Jones potential down to the minimum, although this may not be obvious from the definition of the potential. To prevent the atoms from freezing into a densely packed crystal structure, Dzugutov then introduced a maximum at a distance of about $\sqrt{2} \times r_{nn}$, where r_{nn} is the nearest neighbor distance. The results obtained were different from what Dzugutov originally expected [8]: The structure did not crystallize in the molecular dynamics cooling simulations, but transformed after a very long annealing time of several million time steps into a quasicrystalline structure with layered dodecagonal symmetry.

Principles for determining phase transitions

To determine phase boundaries between two thermodynamic phases precisely one has to compute free energies. This is a quite elaborate task if done by computer simulations. Since I was not interested in the thermodynamic properties of the phases in detail, I started with solid samples and heated them at constant pressure until they melted. The transition temperatures were determined by looking for discontinuities in the potential energy, volume, and mean-square displacements.

It is well known that such a procedure does not yield the true thermodynamic phase transition line but a line where the solid becomes mechanically unstable as a whole. There are at least two reasons for this behavior: first, if periodic boundary conditions are applied, surface melting is suppressed. The system cannot melt continuously and forms a two-phase equilibrium state. Second, since the system is rather small, it cannot develop two competing phases due to the prohibitively high interface energy. Thus the melting transition is delayed. An equivalent retardation of the phase transition takes place if a liquid is cooled: a critical nucleus must be formed, and even large-scale reordering might be necessary. Altogether this implies that a hysteresis loop is observed, and the "real" phase transition takes place at a temperature somewhere within that loop.

Instead of varying the temperature at constant pressure one could also change the pressure at constant temperature. If a liquid is compressed in this way the formation of a solid is delayed, and if a solid is expanded at sufficiently high temperatures the melting is retarded. Again a hysteresis loop is observed instead of a two-phase domain.

At this place some terms may be defined: throughout this paper "liquid" denotes an ordinary condensed liquid if a corresponding "vapor" exists. The mobile phase of the Dzugutov potential is called a "fluid".

The solid structures

The first step in the study of a melting or freezing transition is to find plausible solid structures. From Dzugutov's work [8] it was already known that square-triangle phases should be stable. The generalized structures of this type are formed by assembling squares, triangles, rhombi or shields (Figs. 2 and 3) at random, but without gaps or overlaps. A comparison of different classes of these structures, namely ideal or random dodecagonal quasicrystals, low-order approximants, and crystalline A15, Z, H, and σ-phases (Fig. 4), showed that the σ-phase is the lowest in energy at $T = 0$ and $P = 0$. A search for other solid structures turned out that the crystalline bcc and fcc phases are also competitive at certain pressures [12]. Therefore the σ-phase, fcc and bcc were studied in the simulations.

The σ-phase samples contained 60, 480, and 7500 atoms. The numbers in the bcc crystals amounted to 54, 250 or 1024 atoms, and the fcc crystals used as the starting structures for the simulations with Lennard-Jones potentials had 108 or 500 atoms in the box.

The simulation method

The simulations were carried out with the classical molecular dynamics method. For isothermal (NVT) and isothermal-isobaric (NPT) simulations the constraint method was used [15]. The equations of motion were integrated with a fourth-order Gear-predictor-corrector algorithm (see, for example [15]). The time increment was

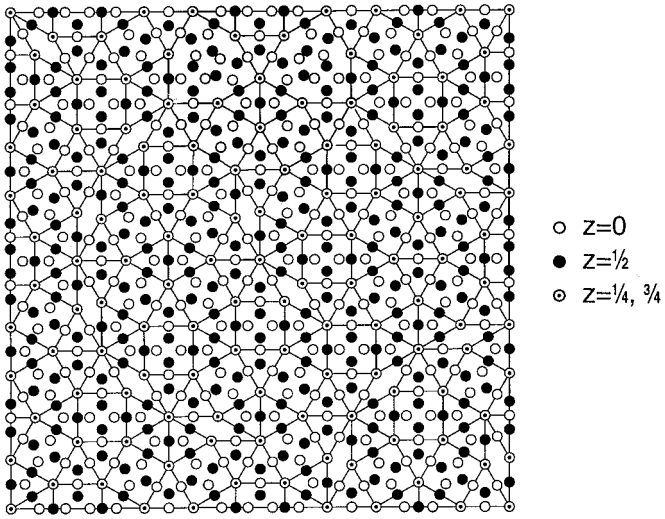

Fig. 2. A dodecagonal random tiling with squares, triangles, rhombi and shields. The different marks indicate the height of the atoms along the periodic z-direction. One z-period is approximately as long as the edge of a tile.

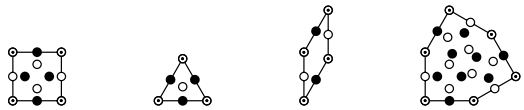

Fig. 3. The basic tiles. From left to right: square, triangle, rhombus and shield. The triangle also occurs in a configuration where the white and black atoms are interchanged. These are all known stable tiles. The marks are the same as in Figure 2.

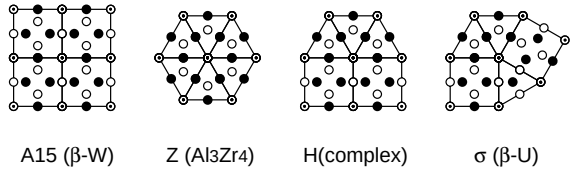

Fig. 4. The vertex configurations which contain only squares and triangles. The patterns also characterize the four crystalline phases noted below the vertex pictures.

$\delta t^* = 0.0005$[1] for all the simulations. The heating and cooling and the compression and expansion simulations were all carried out with constant temperature or pressure gradients, respectively. Constant density and volume gradients were also applied, but such simulations turned out to be rather problematic to carry out. The temperature and pressure gradients will be given with the presentation of the results. The simulation box was cubic, if permitted by the crystal structure, or orthorhombic otherwise, but only isotropic volume changes were permitted. Periodic boundary conditions were applied throughout the simulations.

[1] All results will be given in reduced units [15] and are marked by *. The unit of energy ϵ is the minimum of the Lennard-Jones potential.

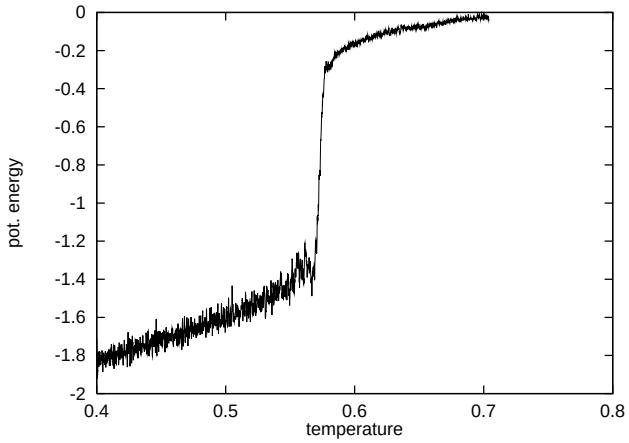

Fig. 5. Phase transition of the σ-phase with the Dzugutov potential. The potential energy is plotted for a heating simulation. The pressure is $P^* = 0.01$, and the temperature gradient $\delta T^* = 0.002$ per time step.

3 Determination of the transition line

In this section the simulation procedures carried out to compute the pressure-temperature phase diagram of the pure Dzugutov potential are described. The transition lines have been determined by heating and cooling at constant temperature and by compressing and expanding at constant pressure.

Heating simulations

Consider an ordinary Lennard-Jones crystal which is heated at low constant pressure. The potential energy at the melting point will jump from about -4 to about -2. At the boiling transition the energy jumps again to about 0. The behavior of the Dzugutov potential is completely different: at the only observable phase transition the potential energy jumps from about -1.4 to -0.2 (see Fig. 5). The volume explodes by an order of magnitude. This clearly indicates that a sublimation transition takes place instead of melting. It is the first hint that there is *no* liquid phase, at least at low pressures. The question remains if a triple point exists, and if the applied pressure was below the triple point pressure.

To find out if the transition behavior changes with increasing pressure the phase boundary for the Dzugutov potential has been traced from $T^* = 0$ to 6 at constant pressures between $P^* = 0$ to 100. The temperature has been increased linearly at a gradient of $\delta T^* = 0.001$ or 0.002 per time step. The bulk of the simulations has been carried out starting from the bcc phase. Further runs have been conducted with the σ-phase and fcc crystals. The transition lines for different structures are rather similar

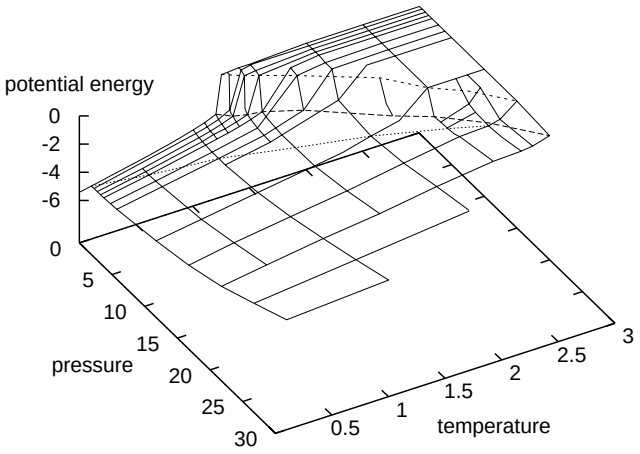

Fig. 6. Potential energy surface *vs.* temperature and pressure. The dotted line indicates a path in a constant-volume simulation starting at the equilibrium volume, the long dashed line marks the onset of the phase transition and the short dashed line its termination. The upper plateau is the potential energy of the fluid phase, the lower surface the potential energy of the solid.

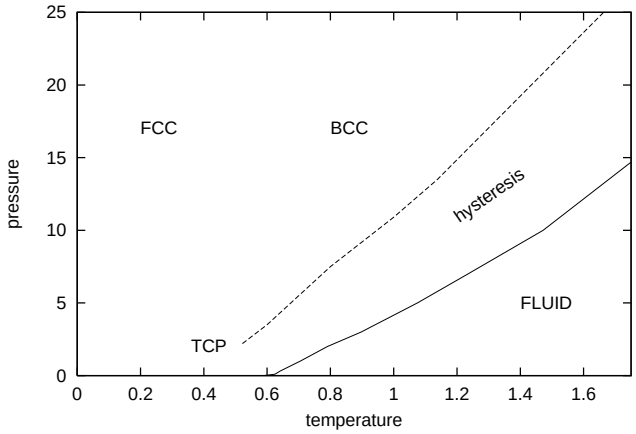

Fig. 7. Schematic pressure-temperature phase diagram. The full line indicates the phase transition obtained by heating and expansion, the dashed line marks the transitions observed by cooling and compression. Between the two lines is the hysteresis region. The phases obtained by cooling are given in capital letters.

in the low pressure range. But at increasing pressure the σ-phase becomes unstable. At even higher pressures the bcc crystals vaporize at lower temperatures compared to the fcc crystals. This indicates that fcc becomes the stable phase at high pressures. Since it is known that fcc is the ground state at high pressures close to $T = 0$ [12] it seems reasonable to assume that fcc is the stable structure for any temperature in this pressure domain. A clear jump of the potential energy and a jump in the volume and density, respectively, occur in the whole range of pressures if the transition line is crossed (see Fig. 6). There is no indication of a two-stage transition first to a liquid and then to a vapor phase at any pressure within the range studied.

To permit a comparison of my results to Dzugutov's work I have determined the transition points of the bcc-, fcc- and σ-phase in constant-volume heating simulations (Fig. 7). The starting samples were equilibrated at $T^* = 0.001$ and $P^* = 0.001$. During the heating the pressure increases continuously and a jump occurs when the heating path crosses the transition line determined with constant-pressure simulations. At first sight the system behaves rather unexpectedly at the transition as the pressure jumps to a value *above* the constant-volume transition line. In the thermodynamic limit one would expect that only a sharp bend in the pressure-temperature path occurs. The reason for the jump is that the onset of the phase transition is delayed stronger than its termination. The end points of the phase transitions at different volumes yield a new transition line in addition to the constant-pressure transition line. This second line reduces the width of the hysteresis region since it lies at lower temperatures compared to the constant-pressure transition line.

Compression and expansion at constant temperature

Up to now the transition line has been traced by heating a solid until it melts or vaporizes. A liquid phase could have been missed if its potential energy difference or the volume change is small. But there exists a second possibility to find the transition line: if a fluid is compressed or a solid is expanded the behavior of the system can be traced in a direction orthogonal to the heating and cooling paths. Again discontinuities are expected to occur if a phase boundary is crossed.

The starting point for these simulations are low-density fluids obtained from previous heating simulations at low pressure. The fluid is compressed continuously at constant temperature. No discontinuity or change in the slope of the density *vs.* pressure function $P^*(\rho)$ is observed until a collapse to the solid takes place. Figure 8 shows $P^*(\rho)$ for temperatures between $T^* = 0.6$ and 4.0. If a liquid phase were present it should modify $P^*(\rho)$ even if it were hidden due to metastability or if it could not be accessed directly due to hysteresis effects. The structure of the solid phase created from the fluid by compression at constant temperature is always the bcc-phase in the temperature range between $T^* = 0.6$ and 4.0. The significance of this result is not that the bcc structure is the stable state in this region of the phase diagram, but only that it is the easiest accessible phase.

Afterwards the solidified structures were expanded again by reducing the pressure at constant temperature. A hysteresis loop similar to the one obtained in the heating and cooling simulations at constant pressure is observed. The transition line where the solid breaks apart is approximately the same as the line obtained by heating simulations. Again no hint of a liquid state is found. The only phase transition observed is the vaporization of the solid. Two separate transitions which could be interpreted as melting and boiling at constant pressure do not occur.

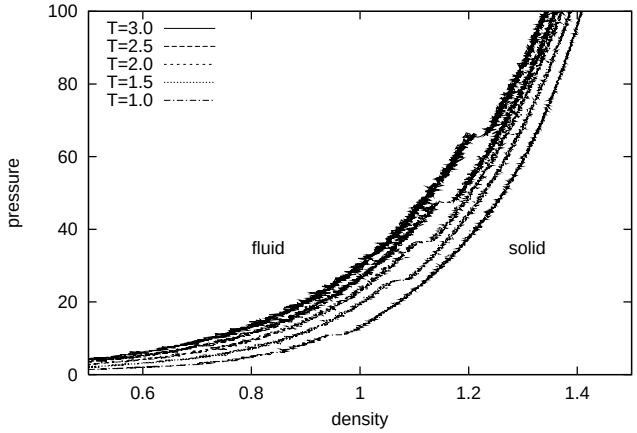

Fig. 8. Compression of the Dzugutov liquid at constant temperatures. From bottom to top, curves correspond to $T^* = 1.0, 1.5, 2.0, 2.5$, and 3.0. The pressure gradient was $\delta P^* = 0.1$ per time step.

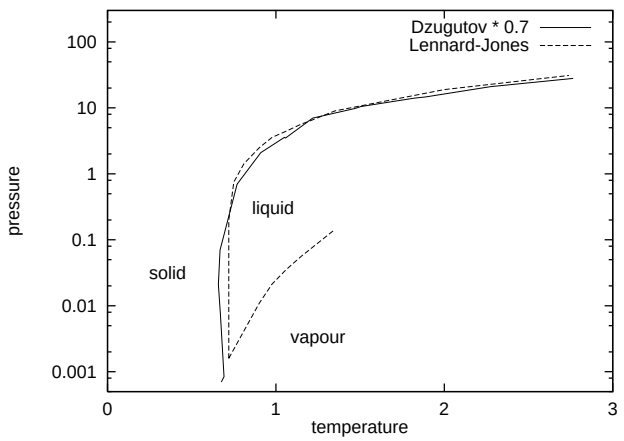

Fig. 9. Comparison of the pressure-temperature phase diagram for the Lennard-Jones potential and for the Dzugutov potential. The Lennard-Jones transition lines are from reference [16].

Cooling simulations

Now the fluids obtained by heating and vaporizing the solids are equilibrated at high temperatures. If the fluids are cooled subsequently at a rate of $\delta T^* = 0.002$ per time step an ordered solid is retained. A more detailed discussion of these simulations may be found in reference [12]. If the pressure is larger than $P^* = 5$ and the size of the sample is small the bcc phase is generated at any cooling rate. But if the size is increased or the pressure is lowered the cooling rate has to be reduced accordingly to get the bcc phase. For 500 atoms δT^* is reduced to 0.0005 and further down to 0.00025 for 1024 atoms. At higher cooling rates an amorphous structure is generated. It is rather surprising that the bcc phase is obtained in the compression and cooling simulations, since the fcc phase seems to be the most stable solid phase at high pressures. A possible explanation has been given already: the bcc crystals may not be the stable structure but only the phase which can readily nucleate. The phase transition to the solid is delayed again due to hysteresis effects. It is approximately the same line as the one observed in the expansion simulations. If the pressure is smaller than about $P^* = 5$, tetrahedrally close packed (tcp) phases [14] are found. The samples contain Frank-Kasper polyhedra as nearest-neighbor coordination shells similar to the quasicrystals obtained by Dzugutov. The square-triangle quasicrystals are actually a special case of perfect Frank-Kasper phases. It is not clear if Dzugutov's structure is only one case of an ensemble of structures, and more general Frank-Kasper phases could be produced by cooling or if the dodecagonal square-triangle quasicrystals are singled out by stability in this region of the phase diagram. In this pressure range the transition to the solid is not well defined. Very low cooling rates and many cooling runs would be necessary to pin down the transition.

The pressure ranges above and below $P^* = 5$ can be translated into corresponding density ranges. In the constant-volume cooling the tcp phase is formed below $\rho = 0.87$ for the samples with 250 atoms. The limiting density grows up to $\rho = 0.84$ for the 1024 atom samples. The cooling rate has to be lowered again for larger samples.

Comparison to Lennard-Jones

How do these results compare to the phase diagram of the Lennard-Jones potential? The heating and expansion phase transition line of the Dzugutov potential can be nicely mapped onto the melting line of the Lennard-Jones system by an appropriate scaling of temperature and pressure by the *same* factor 0.7 (Fig. 9). Due to the hysteresis effects this is not a clean action, but a modified scaling factor should similarly map the true transition line of the Dzugutov potential onto the Lennard-Jones melting line. The mapping property restricts the domain of the pressure-temperature phase diagram where a liquid can be expected for the Dzugutov potential. This region has been investigated thoroughly with our simulations and no trace of a liquid has been found.

4 Mixed potentials

It has been mentioned already that the repulsive part of the Dzugutov potential has been derived from the Lennard-Jones potential. Therefore the forces between nearest-neighbor atoms are identical if the atoms are close enough. The potential energy, however is different, since the Dzugutov potential is shifted with respect to the Lennard-Jones potential (Fig. 1). Phase transitions should occur at slightly different temperatures, since the relationship between the potential energy and the kinetic energy is altered. The pressure-temperature phase diagram of the Lennard-Jones potential is well known, especially the range where the liquid exists. In the previous section I have determined for the Dzugutov the transition

line where the solid becomes unstable. Furthermore it has been pointed out that the melting line of the Lennard-Jones potential and the sublimation line of the Dzugutov potential are rather similar (see Fig. 9). It is therefore natural to search for a connection between the two potentials and their phase diagrams. It would be especially helpful if one could observe a gradual disappearance of the liquid phase. This goal has been achieved by a linear superposition of both potentials. At the two end points of parameter space are the pure Dzugutov potential and the pure Lennard-Jones potential with their phase diagrams. If the contribution of the Dzugutov potential is reduced and the Lennard-Jones part is increased, the maximum of the potential gradually vanishes and the potential range increases. The liquid domain of the Lennard-Jones potential should move to other temperatures or pressures, shrink or otherwise change its shape.

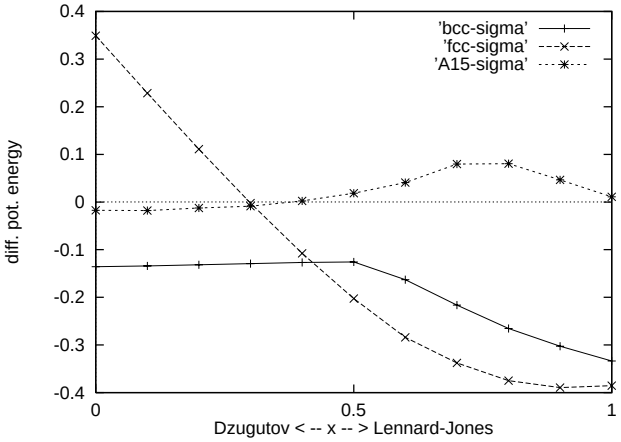

Fig. 10. Potential energy differences of different stable structures at $T = 0$ and $P = 0$ as a function of the mixing factor x.

Results for the mixed potentials

A one-parameter sequence of potentials has been generated by a linear superposition of the Dzugutov and the Lennard-Jones potentials: $V(r) = xV_{\mathrm{LJ}}(r)+(1-x)V_{\mathrm{Dz}}(r)$. If the fraction x is 0 the pure Dzugutov potential is retained, and at $x = 1$ the ordinary Lennard-Jones potential is present.

The first step to studying the mixed potentials, is to test the reaction of the stable structures with the pure Dzugutov potential [12] and the pure Lennard-Jones potential. These are bcc, fcc and the σ-phase. As an additional example of a square-triangle phase the A15-phase has been studied. For the Lennard-Jones potential the ground state at $T = 0$ is hcp, but fcc is only marginally less stable. For simplicity, the fcc structure has been used.

At $T = 0$ and $P = 0$ the Helmholtz free energy F, the Gibbs free energy G, the internal energy U, the enthalpy H, and the potential energy E_{pot} become identical. Therefore it is adequate to use the potential energy as a measure of the stability of the different phases. For numerical reasons temperatures and pressures can not be set to zero exactly, thus the simulations were carried out at very low temperatures and pressures. A comparison of the potential energies for the mixed potentials at $T^* = 0.001$ and $P^* = 0.001$ shows that the most stable solid structure is the bcc phase for $x < 0.3$ and the fcc phase for $x > 0.3$ (Fig. 10). The A15-phase is similar to the σ-phase, but both are less stable than bcc and fcc for any x.

If the temperature is larger than zero, the entropy and the kinetic energy start to play a role in the stability. The kinetic energy, however, is the same for all x at a certain temperature, thus its contribution can be neglected. Since the free energy has not been calculated explicitly, it is not clear how the stability of bcc and fcc changes at higher temperatures. The potential energy may be used as a rough guideline if it is assumed that the contribution of the entropy to both phases is similar. The fraction x where the potential energies of bcc and fcc are equal, shifts from $x = 0.3$ at $T = 0$ to $x = 0.4$ at the phase transition temperature. With the previous assumptions this implies

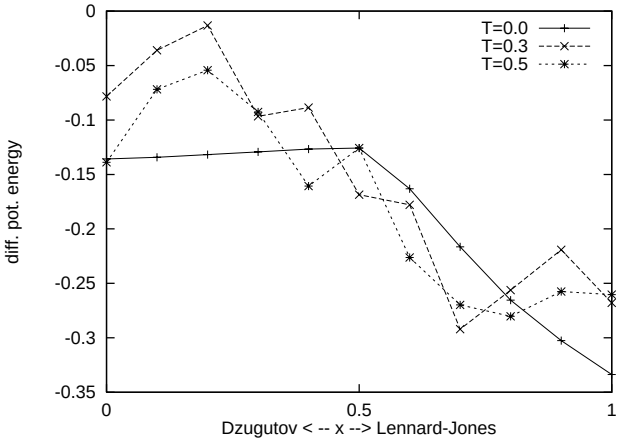

Fig. 11. Potential energy differences between bcc and the σ-phase as a function of the mixing factor x at different temperatures. The lines are only guides to the eye.

that the stability at $x = 0.35$, for example, changes from fcc to bcc with increasing temperature. The difference in potential energies between bcc and the σ phase is small, but the bcc phase is always lower than the σ-phase for all x. The difference increases if the potential is more like Lennard-Jones (Fig. 11). If the σ-phase is used as a starting structure for a heating simulation it is observed that it becomes unstable at about $T^* = 0.5$ to 0.58 if x is larger than about 0.4 (see Fig. 12). Sometimes the solid melts and sometimes it transforms into the stable fcc structure.

Heating simulations

The second step comprises heating simulations at different x and P^* values. Figure 13 shows the potential energy curves for the σ-phase at different x and low pressure. For $x = 0$ only one transition occurs. A two-step phase transition sets in at $x = 0.5$ and is clearly visible for $x = 0.7$ and $x = 0.8$. For $x = 1$ no two-step transition can be

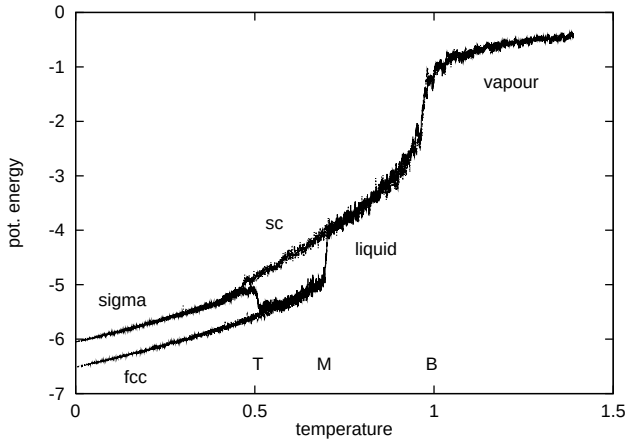

Fig. 12. Potential energies obtained in heating simulations for a potential close to the pure Lennard-Jones case ($x = 0.9$). The pressure is $P^* = 0.01$, the temperature gradient $\delta T^* = 0.002$ per time step. The labels T, M and B indicate the transition from the σ-phase to a supercooled liquid (sc) or fcc (T), the melting transition (M), and the boiling transition (B).

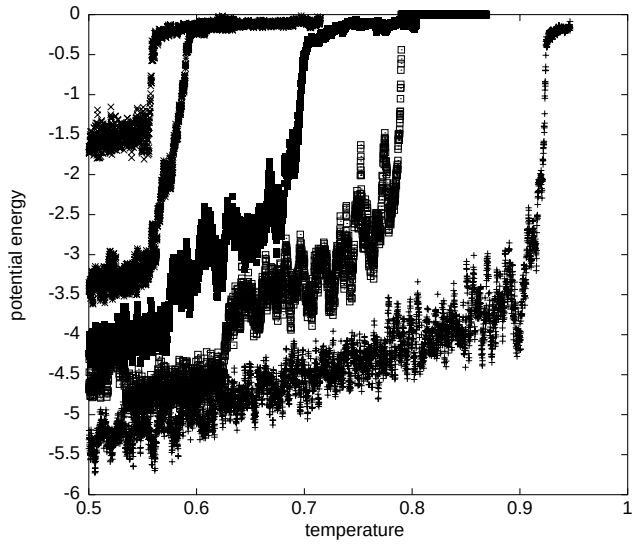

Fig. 13. Potential energies obtained in heating simulations of the bcc phase with different mixed potentials. The curves are from left to right: $x = 0$, 0.5, 0.7, 0.8, 1.0. The upper jump marks the transition to the vapor phase. For $x = 0.5$ to 0.8, the development of a second jump can be seen clearly at about $T = 0.6$. This indicates a solid-liquid transition. At $x = 1.0$ the bcc structure is unstable, therefore no transition to a liquid is observed.

found since the σ-phase is unstable and decays already at $T^* = 0.58$.

Now the transition behavior at fixed pressure is presented as a function of x. At $P^* = 0.01$ and x between 0 (Dzugutov) and 0.4 a transition from the solid to a low-density fluid (Fig. 14) is observed. The transition is only weakly dependent on the applied pressure up to $P^* = 0.1$, but shifts to higher T^* if P^* is increased to $P^* = 1.0$ and

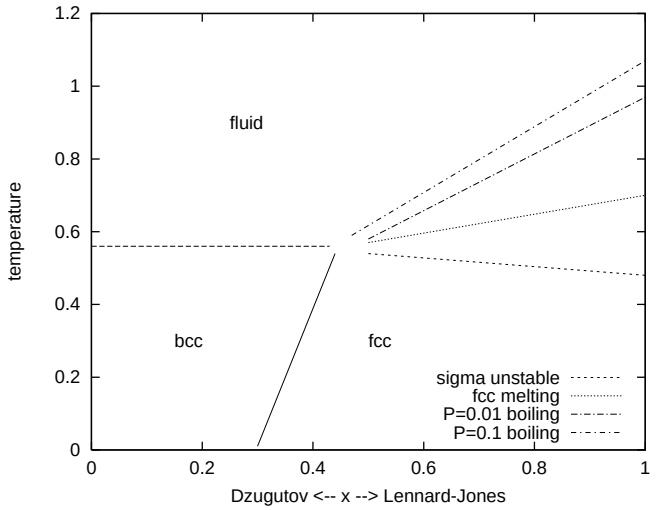

Fig. 14. Mixing-temperature-diagram. Low x: transition from the bcc solid to a fluid for $P^* = 0.01 - 0.1$. Large x, from bottom to top: instability line of σ-phase, melting line of fcc phase, boiling lines at $P^* = 0.01$ and 0.1. The topology of the intersections in the center of the plot cannot be derived from the simulations.

further to $P^* = 10.0$. The dependence of the transition line on x is weak but increases for higher pressures. The phase diagram is similar to the Dzugutov case at $x = 0$: only one fluid phase is present. On the contrary a transition from the solid to the liquid and further to the vapor is observed at $x = 1$ (Lennard-Jones). If x is reduced from 1 to 0.4, the melting temperature decreases weakly but the boiling temperature falls rapidly. At about $x = 0.4$ both lines meet and the liquid disappears. Since the sublimation line remains at constant temperature if x is increased from 0 to 0.4 it meets the other melting and boiling lines at about $x = 0.4$ (Fig. 14). For large x the boiling transition line depends more strongly on the applied pressure. The line shifts to higher temperatures even if P^* is still in the range between $P^* = 0.1$ and 0.01. At larger pressures (for example $P^* = 1.0$ and 10.0) the system is above the critical temperature of the Lennard-Jones system for $x = 1$ (Fig. 9), and the liquid phase of the Lennard-Jones potential disappears. The same happens for x between 0.4 and 1.0. Since no liquid phase existed for x between 0.0 and 0.4 a common sublimation line ranging from $x = 0$ to 1 is obtained. This line shifts gradually to higher temperatures if the pressure is increased further (Fig. 14).

It is also illustrative to consider what happens with the transition lines in the pressure-temperature phase diagram if x is varied. The solid-vapor transition line below the triple point does not change much in the whole range between $x = 0$ and $x = 1$. The solid-liquid and the solid-fluid transition lines shift to slightly smaller temperatures. The liquid-vapor transition line, however, changes considerably: if x is lowered from 1 to 0.4 it shifts towards the solid-liquid transition line and finally vanishes at x about 0.4 (see Fig. 15). This is the most conclusive test that there is no stable liquid phase for the Dzugutov potential.

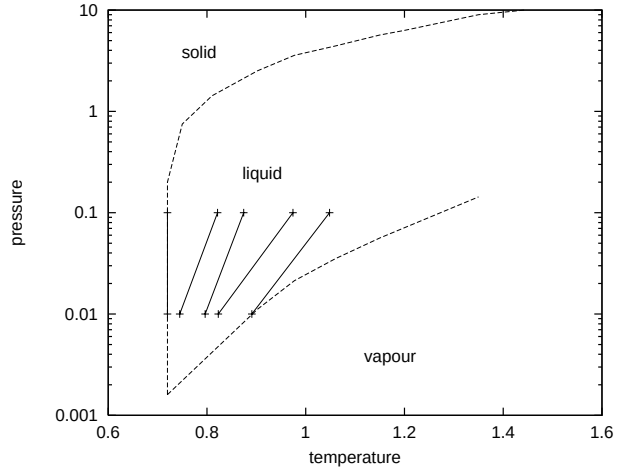

Fig. 15. Pressure-temperature phase diagram. Full lines: boiling transition lines of the mixed potentials. From left to right: $x = 0.6$, 0.7,0.8, 0.9 1.0. The temperatures have been scaled with the melting temperatures to simplify the diagram; otherwise the melting lines would move to lower temperatures for smaller x as can been seen by comparison with Figure 14. Dashed lines: transition lines of the pure Lennard-Jones potential from reference [16].

This behavior is the same as that occurring for the other potentials studied so far [1–6].

Compression simulations

In a final study low density fluids were compressed at a constant temperature $T^* = 1.0$. In the Lennard-Jones case ($x = 1.0$) two phase transitions are observed since the starting point is below the boiling temperature (see Fig. 15): first the collapse of the vapor to a liquid occurs and then the solidification of the liquid sets in. On the contrary only a single transition is present in the Dzugutov case ($x = 0.0$). The collapse from the vapor to the fluid is shown in Figure 16 for a compression rate of $\delta P^* = 0.001$ per time step. The solidification which occurs at about $P^* = 20$ is not shown. The different behavior for $x = 0.0$ and $x = 1.0$ is obvious. For $x = 0.8$ the jump in density from the vapor to the liquid is already smeared out considerably, and lower compression rates would be necessary to resolve the transition clearly. This trend worsens for lower x. The compression at constant temperature therefore confirms the phase diagram (Fig. 14) derived from the heating simulations: there is no liquid phase for low x.

Density vs. temperature

If the phase boundaries of the vapor-liquid transition are plotted as a function of temperature and density and with the potential mixing ratio x as a parameter (Fig. 17) the gradual disappearance of the distinction between vapor and liquid with decreasing x can be seen directly. At $x = 0.6$ and $x = 0.5$ the coexistence region has become so narrow that variation of the transition at different runs is larger than the width of the liquid region. For a specific run, however, the two-step transition vapor-liquid-solid is still observable.

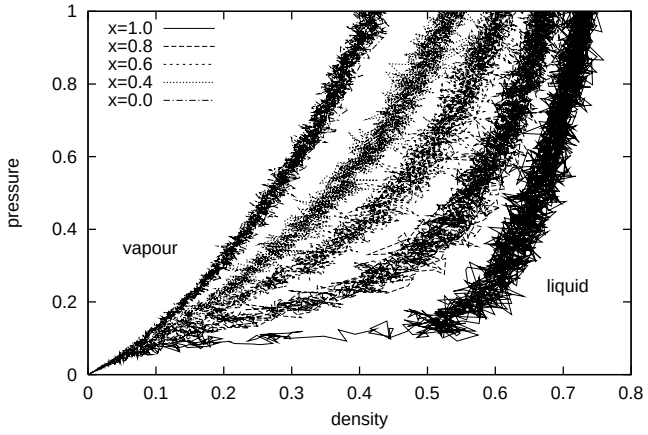

Fig. 16. Pressure *vs.* density for mixed potentials with $0 < x < 1$. The vapor is compressed at a rate of $\delta P^* = 0.001$ per time step. From left to right: $x = 0.0$, 0.4, 0.6, 0.8, 1.0. The vapor-liquid transition is visible for $x = 1.0$ as a horizontal jump. It is smeared out for $x = 0.8$, and vanishes gradually as x is reduced down to $x = 0.0$.

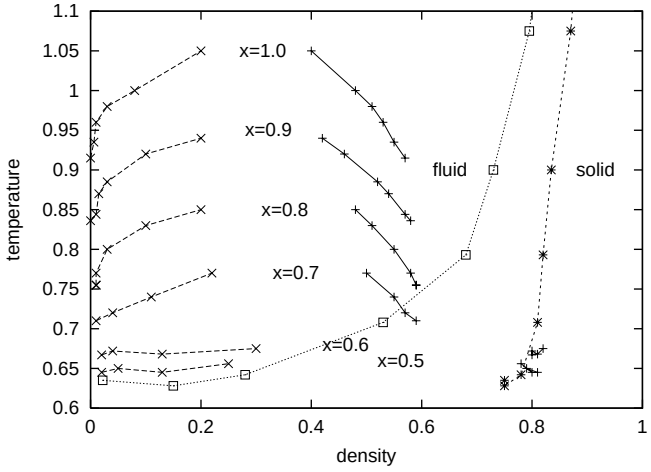

Fig. 17. Temperature *vs.* density for mixed potentials with $0 < x < 1$. The crosses and pluses indicate the vapor-liquid transition. The boxes and stars mark the boundary of the fluid-solid (fcc) transition. At $x = 0.6$ and $x = 0.5$ the coexistence region has become so narrow that it is not visible any more.

5 Discussion and conclusion

The results presented in this paper indicate that a liquid phase is not present in the phase diagram of the pure Dzugutov potential. If the Dzugutov potential is superimposed linearly with the Lennard-Jones potential a liquid phase is observed until the fraction of the Dzugutov potential x becomes smaller than $x = 0.4$. The liquid phase of

the Lennard-Jones potential does not shift to higher temperatures or other pressures if x is lowered from 1 to 0.4, but shrinks continuously, and finally vanishes completely at $x = 0.4$ (Fig. 14).

The results fit well into the overall scheme of phase diagrams without a liquid phase. The attractive well of the Dzugutov potential is at a distance of about $r = 1.3$ and the potential range is $r = 1.94$, so the interaction is rather short ranged. The potentials obtained by superimposing the Lennard-Jones and the Dzugutov potential may have a second, very shallow minimum which does not influence the phase diagram since it is at least an order of magnitude less attractive than the first minimum. But what really plays a rôle is the maximum at about $r = 1.6$. To surmount this obstacle the temperature of the atoms has to be rather high. In the Lennard-Jones case the bonds between the atoms get continuously weaker if their kinetic energy increases with raising the temperature. An atom becomes unbound if its kinetic energy is high enough to overcome the binding energy. At this point, the large kinetic energy with respect to infinity and the interaction is still attractive, therefore a liquid is formed. In the Dzugutov case an atom has to gain much more kinetic energy to become unbound since the difference between the minimum and maximum energy determines the attraction. But if an atom finally is free it has a large kinetic energy with respect to infinity, and the interaction is now purely repulsive. The atoms will therefore collide with high energy and separate again immediately. The result is a vapor phase instead of a liquid. With increasing Lennard-Jones contribution the maximum of the potential gets flatter. The kinetic energy necessary to break an atom out of the crystal lattice becomes smaller and the surplus kinetic energy reduces also. If the maximum is low enough, the existence of a liquid phase becomes possible.

Now the case of continuous cooling or compression of a vapor is considered. Atoms interacting *via* a Lennard-Jones potential will get closer and closer with falling temperature since there exists no repulsive barrier between the atoms. Finally a liquid or an amorphous phase will form at any pressure above the triple point if the temperature has become low enough. Thus it is easy to form a condensed phase. Atoms interacting *via* the Dzugutov potential will repel each other if cooled, starting from a high temperature – low pressure state. From time to time two atoms get trapped by each other if they lose their kinetic energy in the right moment of a collision, but most often the atoms will collide and separate again. Therefore we need high pressure and low cooling rates to produce a condensed phase. Otherwise a low-temperature vapor phase which resembles a foam will be formed.

A further explanation of the phase diagram is obtained by looking at the potential itself and relating it to the binding energy. The potential has been constructed in such a way that the energy barrier (difference between minimum and maximum) is about 1 for all x. If we increase x from 0 to 1 we find that the minimum decreases from -0.58 to -1.00. The binding energy at temperatures below the melting point increases proportionally to the potential minimum. The melting temperature does not change much between $x = 0$ and 1. The melting therefore occurs after the binding energy has changed by the same amount for all x and the mean atomic displacement is about the same. Thus the Lindemann criterion is fulfilled. The drop of the binding energy remains constant if x decreases from 1 to 0.4. This behavior can be explained if the low temperature liquid has a similar structure for these mixed parameters which can be demonstrated by computing the radial distribution functions.

Since the jump of the binding energy at the boiling line reduces only slightly with decreasing x, but the total binding energy decreases also (as explained above), we find that the difference between the binding energies of the low and the high temperature liquid becomes rapidly smaller with decreasing x. If a liquid would exist at x less than 0.4 then the jump at the boiling temperature would have to be less than one energy unit!

Finally, at $x = 0$ we cannot expect the existence of a liquid phase since the potential is very short ranged and only nearest neighbors contribute to the binding energy. In addition we have a maximum which leads to a repulsion of the atoms. Both properties separately would already be enough to avoid a liquid phase.

In this study I have gathered evidence that the Dzugutov potential belongs to the class of short-ranged potentials without a liquid phase. The ongoing discussion of the C_{60} phase diagram [13], however, makes it clear that it is nontrivial to distinguish a stable liquid phase from a metastable fluid. In the case of C_{60}, different simulation methods and density function calculation yield qualitatively different phase diagrams. Since I have not determined the phase boundaries exactly (I used small systems which may exhibit large finite size effects and did not calculate the free energies), I cannot exclude completely that a small liquid range may exist in the hysteresis region between melting and sublimation. But the sharp jumps of potential energy and specific volume observed, if one goes from the fluid to the solid phase, seem to exclude this possibility. Density functional calculations carried out by Denton [17] have confirmed that the liquid state is indeed only metastable.

A comparison of the stability of plausible candidate structures for the solid state [12] has shown that the phase diagram of the Dzugutov potential may not be as simple as one could expect from related potentials (Lennard-Jones for example). There are at least three (meta-)stable structures at temperatures close to $T = 0$. With increasing pressure they are: bcc, the σ-phase and fcc. On the other hand it could not be proven up to now that the dodecagonal quasicrystal discovered by Dzugutov represents a stable state of his potential at higher temperatures. For the colloids this implies that it is still difficult, if not impossible, to create a macroscopic quasicrystal. The Dzugutov potential may be a starting point, but it has to be modified if a stable quasicrystal is to be produced. The absence of the liquid phase is not so important in this case since by increasing the pressure a dense fluid of arbitrary density can be formed.

The author thanks Prof. Dr. H.-R. Trebin, A. Denton and J. Stelzer for helpful discussions.

References

1. A. Daanoun, C.F. Tejero, M. Baus, Phys. Rev. E **50**, 2913 (1994).
2. C.F. Tejero, M. Baus, Phys. Rev. E **48** 3793 (1993).
3. C.F. Tejero, A. Daanoun, H.N.W. Lekkerkerker, M. Baus, Phys. Rev. Lett. **73** 752 (1994).
4. M.H.J. Hagen, D. Frenkel, J. Chem. Phys. **101** 4093 (1994).
5. P. Bolhuis, D. Frenkel, Phys. Rev. Lett. **72** 2211 (1994).
6. P. Bulhuis, M. Hagen, D. Frenkel, Phys. Rev. E **50** 4880 (1992).
7. M. Dzugutov, Phys. Rev. A **46** R2984 (1992).
8. M. Dzugutov, Phys. Rev. Lett. **70** 2924 (1993).
9. J. Roth, C.L. Henley, Phil. Mag. A **75** 861 (1997).
10. F. Gähler, J. Roth, in *Aperiodic '94*, edited by G. Chapnis and W. Paciorek (World Scientific, Singapore, 1995), pp. 183-187.
11. J. Roth, F. Gähler, Eur. Phys. J. B **6**, 425 (1998).
12. J. Roth, A. Denton, *The solid phase structures of the Dzugutov potential*, submitted to Phys. Rev. E.
13. J.Q. Broughton, J.V. Lill, J.K. Johnson, Phys. Rev. B **55** 2808 (1997).
14. D.P. Shoemaker, C.B. Shoemaker, *Icosahedral coordination in metallic crystals*, in *Introduction to quasicrystals* edited by M.V. Jarić, *Vol. 1 of Aperiodicity and order* (Academic Press, Boston, 1988), Chap. 1, pp. 1–57.
15. M.P. Allen, D.J. Tildesley, *Computer Simulations of Liquids* (Oxford Science Publications, 1987).
16. J.J. Nicolas, K.E. Gubbins, W.B. Streett, D.J. Tildesley, Mol. Phys. **37**, 1429 (1979).
17. A.R. Denton (private communication).